

Electronic Supplementary Information

Ni^{II}-Ln^{III} complexes with o-vanillin as main ligand: syntheses, structures, magnetic and magnetocaloric properties

Jean-Pierre Costes, Françoise Dahan, Laure Vendier, Sergiu Shova, Giulia Lorusso, Marco Evangelisti

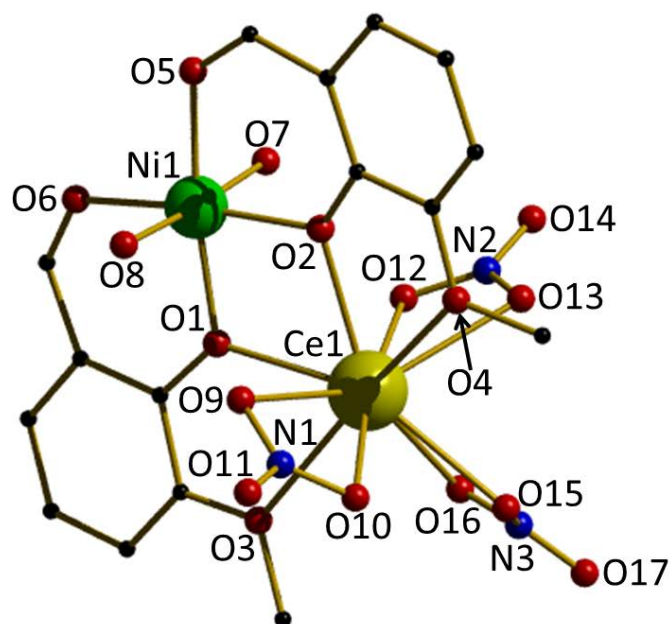


Figure S1. Molecular structure of **2** with atom numbering. Hydrogen atoms are omitted for clarity. Selected bond lengths and angles: Ni-O1 2.007(2), Ni-O2 2.003(2), Ni-O5 2.005(2), Ni-O6 2.007(2), Ni-O7 2.076(2), Ni-O8 2.071(2), Ce-O1 2.423(2), Ce-O2 2.425(2), Ce-O3 2.629(2), Ce-O4 2.600(2), Ce-O9 2.615(2), Ce-O10 2.578(2), Ce-O12 2.612(2), Ce-O13 2.652(2), Ce-O15 2.571(2), Ce-O16 2.613(2) Å, O1 Ni O2 80.86(7), O1 Ce O2 64.88(6), Ni O1 Ce 107.07(7), Ni O2 Ce 107.17(7)°.

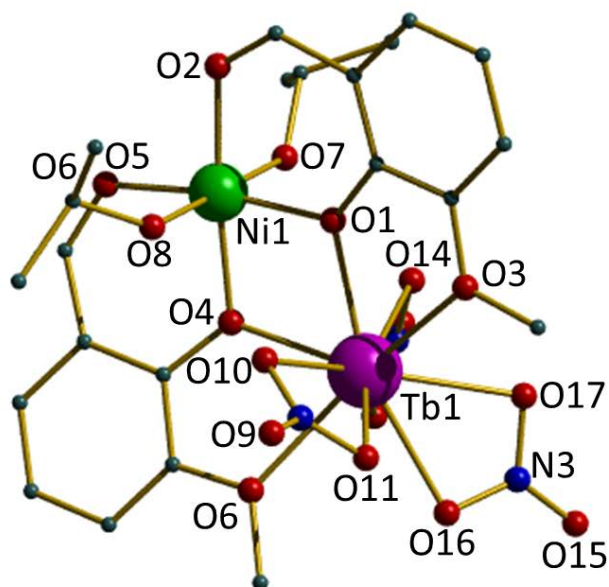


Figure S2. Molecular structure of **3** with atom numbering. Hydrogen atoms are omitted for clarity. Selected bond lengths and angles: Ni-O1 1.997(2), Ni-O2 1.998(2), Ni-O4 2.005(2), Ni-O5 2.003(2), Ni-O7 2.079(3), Ni-O8 2.077(3), Tb-O1 2.353(2), Tb-O2 2.425(2), Tb-O3 2.543(2), Tb-O4 2.332(2), Tb-O10 2.435(3), Tb-O11 2.517(3), Tb-O13 2.507(2), Tb-O14 2.481(3), Tb-O16 2.487(3), Tb-O17 2.498(3) Å, O1 Ni O4 78.44(9), O1 Tb O4 65.38(7), Ni O1 Tb 107.82(9), Ni O2 Tb 108.31(9)°.

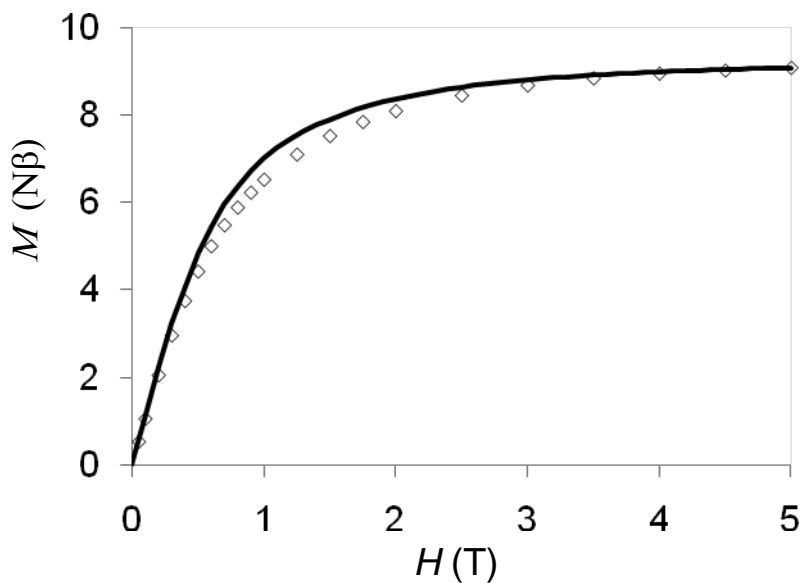


Figure S3. Field dependence of the magnetization for complex **4** at $T = 2$ K. The solid line corresponds to the best fit described in the text with $J_{\text{NiGd}} = 2.48 \text{ cm}^{-1}$, $D_{\text{Ni}} = 4.7 \text{ cm}^{-1}$ and $g = 2.05$.

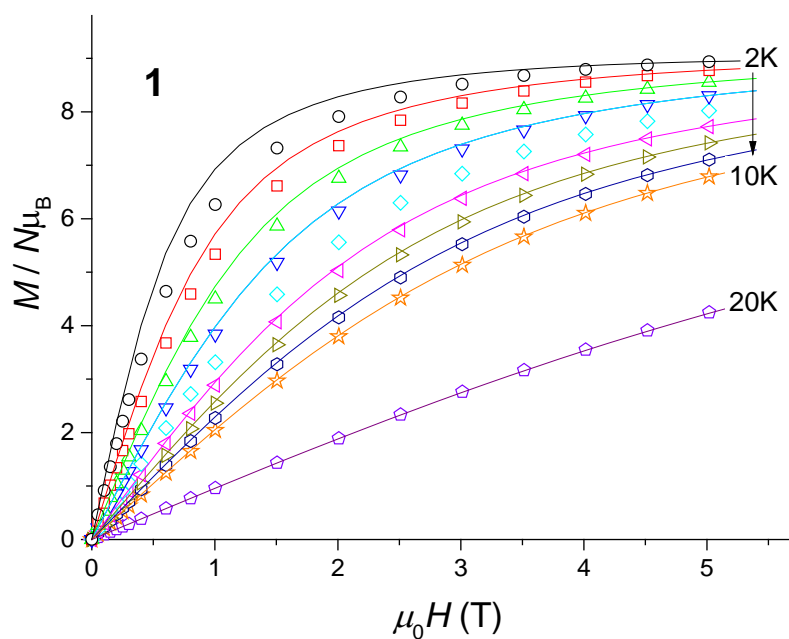


Figure S4. Field dependence of the magnetization for complex **1** at $T = 2$ K. The solid line corresponds to the best fit described in the text with $J_{\text{NiGd}} = 2.77 \text{ cm}^{-1}$, $D_{\text{Ni}} = 2.8 \text{ cm}^{-1}$, $g = 2.03$, without the zJ term.

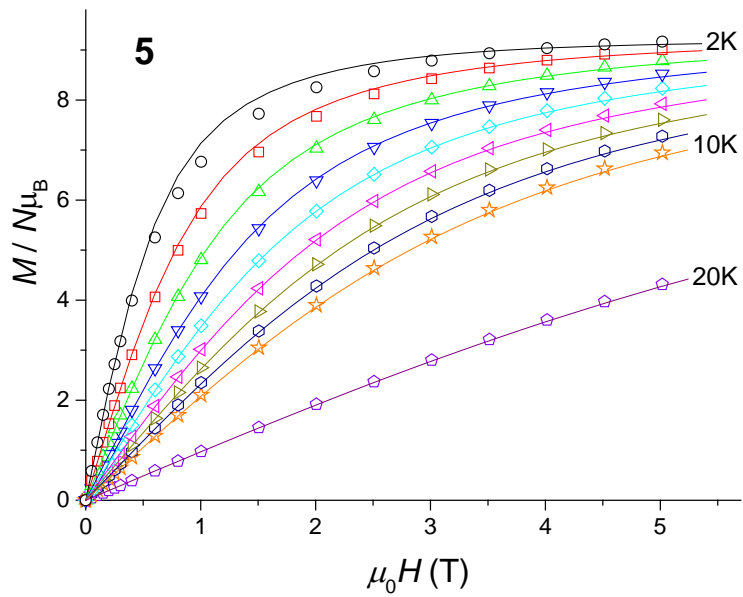


Figure S5. Field dependence of the magnetization for complex **5** at $T = 2\text{--}10$ K, step 1 K and 20 K. The solid lines correspond to the best fit described in the text with $J_{\text{NiGd}} = 2.31 \text{ cm}^{-1}$, $D_{\text{Ni}} = 0.7 \text{ cm}^{-1}$ and $g = 2.04$.

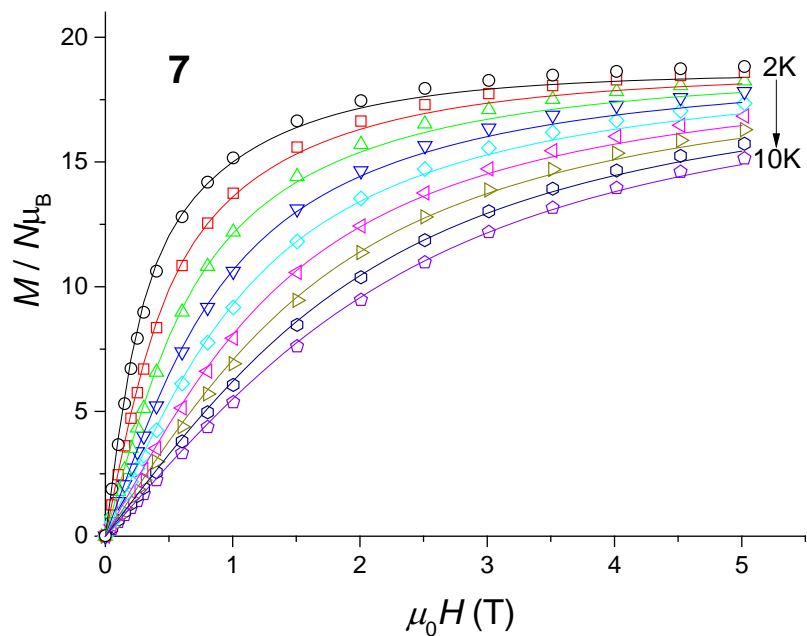


Figure S6. Field dependence of the magnetization for complex **7** at $T = 2\text{--}10$ K, step 1 K. The solid lines correspond to the best fit described in the text with $J_{\text{NiNi}} = 43.8 \text{ cm}^{-1}$, $J_{\text{NiGd}} = 1.21 \text{ cm}^{-1}$, $g = 2.06$ and $D_{\text{Ni}} = 5.8 \text{ cm}^{-1}$.

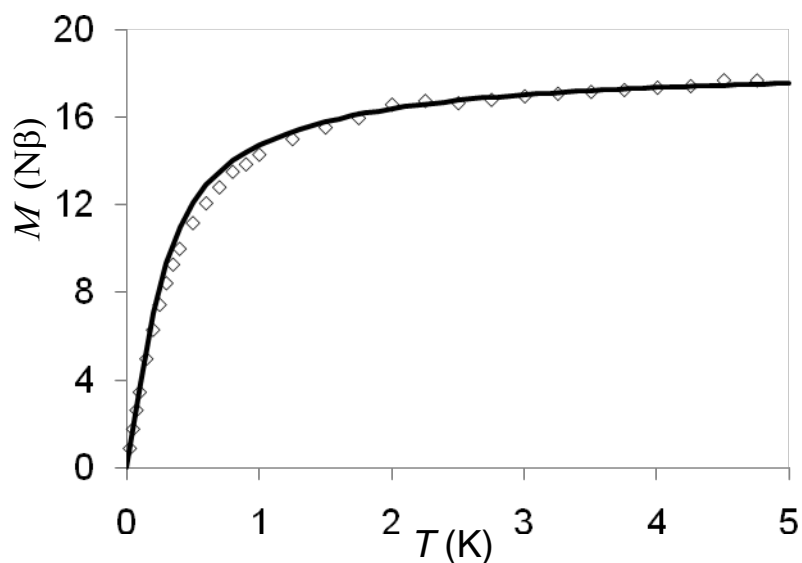


Figure S7. Field dependence of the magnetization for complex **8** at $T = 2$ K. The solid line corresponds to the best fit described in the text with $J_{\text{NiNi}} = 25.0 \text{ cm}^{-1}$, $J_{\text{NiGd}} = 1.40 \text{ cm}^{-1}$, $g = 2.00$, $D_{\text{Ni}} = 5.5 \text{ cm}^{-1}$, without the zJ term.

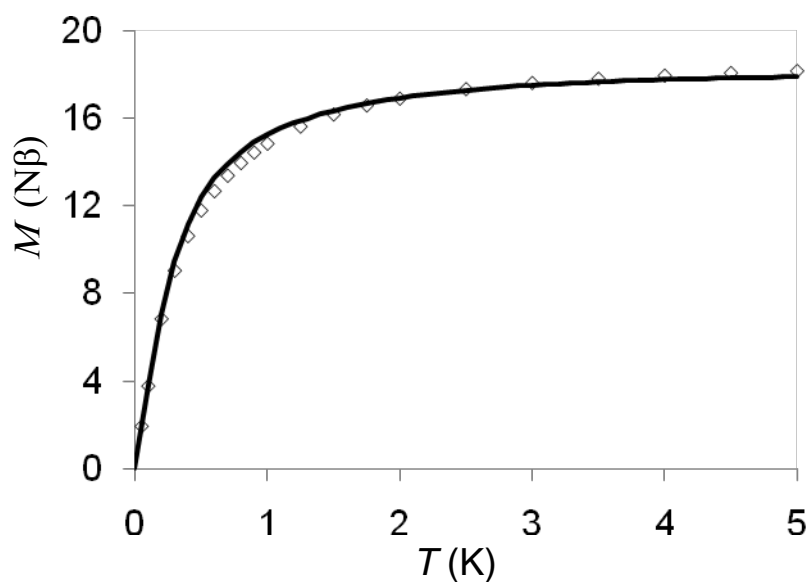


Figure S8. Field dependence of the magnetization for complex **9** at $T = 2$ K. The solid line corresponds to the best fit described in the text with $J_{\text{NiNi}} = 33.8 \text{ cm}^{-1}$, $J_{\text{NiGd}} = 1.12 \text{ cm}^{-1}$, $g = 2.01$ and $D_{\text{Ni}} = 5.5 \text{ cm}^{-1}$.

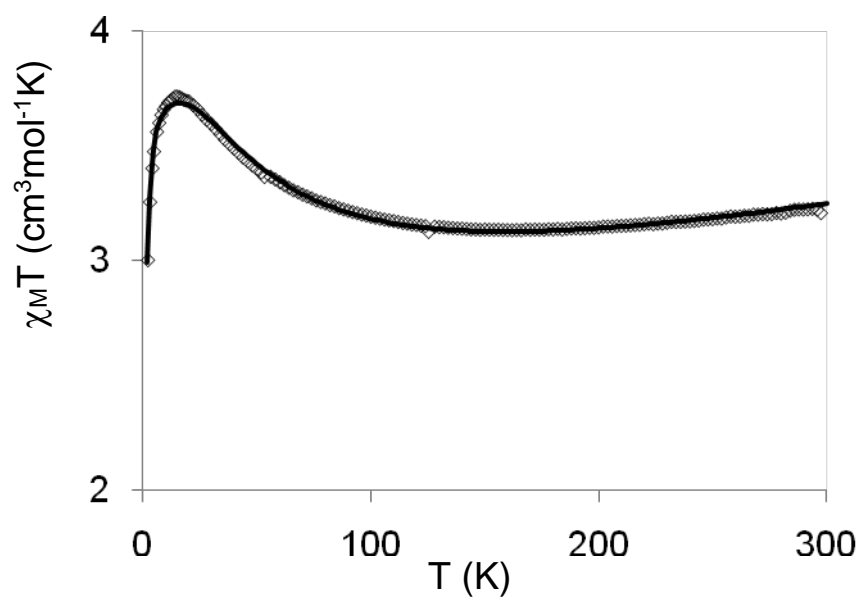


Figure S9. Temperature dependence of the $\chi_M T$ product for complex **10**. The solid line corresponds to $J_{\text{NiNi}} = 25.0 \text{ cm}^{-1}$, $g = 2.22$ and $D_{\text{Ni}} = 5.4 \text{ cm}^{-1}$.

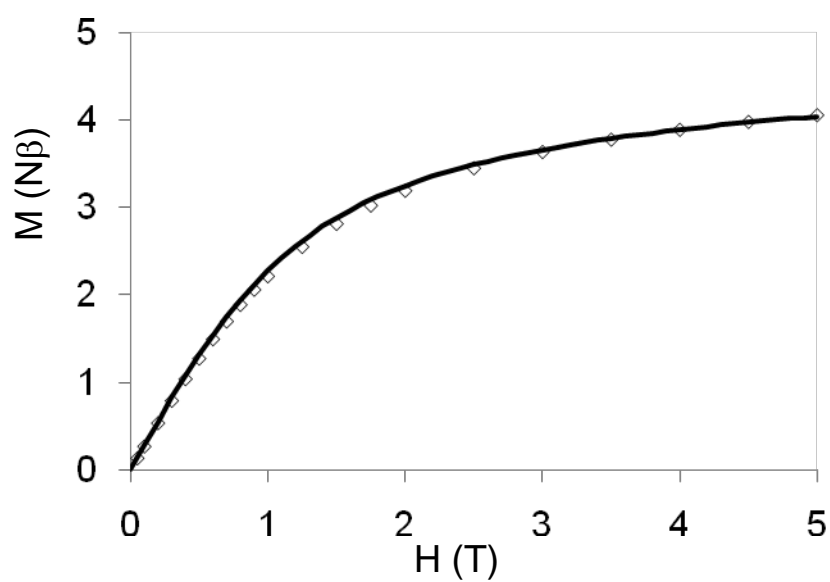


Figure S10. Field dependence of the magnetization for complex **10** at $T = 2 \text{ K}$. The solid line corresponds to the best fit described in the text with $J_{\text{NiNi}} = 25.0 \text{ cm}^{-1}$, $g = 2.22$ and $D_{\text{Ni}} = 5.4 \text{ cm}^{-1}$.

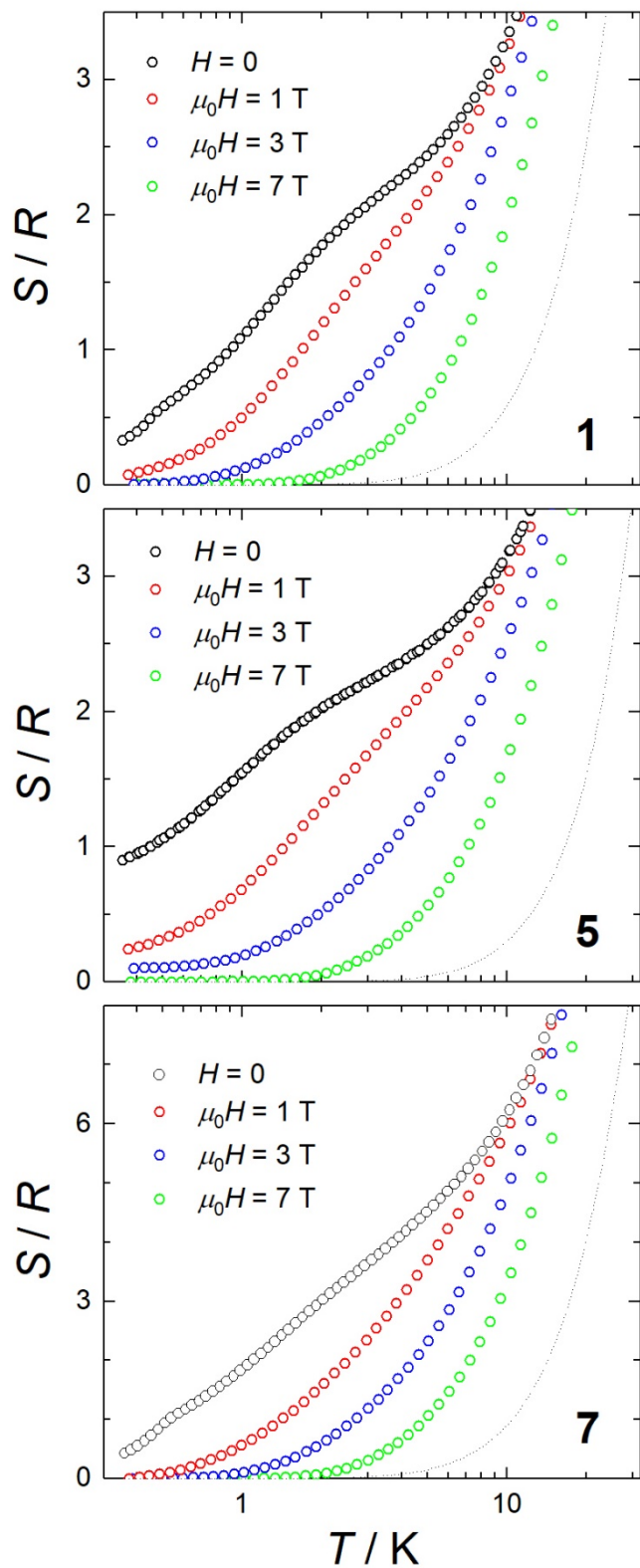


Figure S11. From top to bottom (for complexes **1**, **5** and **7**, respectively): Temperature-dependence of the entropy normalized to the gas constant, S/R , for the indicated applied field changes. Dotted line is the non-magnetic lattice contribution to the entropy.